Mathematics and Statistics: Open Access
Received: Dec 28, 2015, Accepted: Mar 04, 2016, Published: Mar 07, 2016
Math Stat, Volume 2, Issue 1
http://crescopublications.org/pdf/msoa/MSOA-2-008.pdf
Article Number: MSOA-2-008

Research Article Open Access

Transitional Compression Waves from Spherical and Cylindrical Cavities

Ibragim Palankoev*

***Corresponding Author:** Ibragim Palankoev, Russia, E-mail: mishkenzia@gmail.com

Citation: Ibragim Palankoev (2016) Transitional Compression Waves from Spherical and Cylindrical Cavities. Math Stat 2: 008.

Abstract

The present investigations were carried out at the pilot stand, which studies the mechanism of influence of strait blasting waves on the borehole circuit. Under consideration are the transient compression waves from the spherical oscillator in an isotropic elastic medium. Was supposed, that the pressure on the cavity`s circuit is equal in the same intervals. It is intended as a first step to the comprehension of the phenomena taking place around a borehole after the detonation of the charge but before the return of the reflected waves. The paper deals with the transient compression wave emanating from a spherical or cylindrical cavity to the surrounding isotopic elastic solid. It is supposed that the pressure at the boundary surface of the cavity is the same all over, depending only on the time. This supposition, however, only agrees with real circumstances if both cavity and charge are spheres with the ignition point for a centre. This is a consequence of the fact that the velocity of sound in stone (about 5000 m/sec) is not negligible compared with the velocity of detonation of the charge (dynamite LFB slow speed 2500m/sec, high speed 6300m/sec, blasting gelatin 7800 m/sec).

Keywords: Blasting waves; The spherical oscillator; Transient compression wave; Rock blasting.

Introduction

The mechanical treatment of the problems considered does not present essential difficulties. The results are communicated in diagrams showing radial, tangential, axial and maximum shear stresses for different pressure functions and for various distances from centre of the cavity[1]. It appears from the diagrams that considerable tensional stress will rapidly arise in the tangential direction if the solid is submitted to a pure pressure from the cavity. A consequence of these stresses is the appearance of a radial system of cracks around the borehole – the first phase in rock blasting. At greater distances radial tension stresses will also arise but for homogeneous rock masses these stresses will presumably be a little importance. .

Transient Wave from a Spherical Cavity

We consider the infinite solid

$$r>r_0,\ r=\sqrt{x^2+y^2+z^2}$$

Surrounding the spherical cavity $r<r_0$. At the time $t=0$ the solid will be supposed to be in the unstressed state and at rest. After this time we suppose a uniformly distributed normal pressure $P(t)$ acting on the boundary surface $r=r_0$.
E, υ and ϱ denoting modulus of elasticity, Poisson`s ratio and density, respectively, we put

$$\lambda=\frac{\nu E}{(1+\nu)(1-2\nu)}$$

$$\mu=\frac{E}{2(1+\nu)}$$

Then, the sound velocity

$$c=\sqrt{\frac{\lambda+2\mu}{\varrho}}$$

Let u_r be the displacement along the radius vector *(x,y,z)*, σ_r the redial stress. Putting

$$\theta = \frac{1}{r^2}\frac{\partial(r^2 u_r)}{\partial r} \qquad (1)$$

We get

$$\sigma_r = (\lambda + 2\mu)\theta - \frac{4\mu}{r}u_r \quad (2)$$

Now θ satisfied the wave equation

$$\frac{\partial^2}{\partial r^2}(r\theta) = \frac{1}{c^2}\frac{\partial^2}{\partial t^2}(r\theta)$$

Hence

$$\theta = \frac{\varphi(t-\frac{r-r_0}{c})}{r} \qquad (3)$$

And φ*(t)* obviously vanished for *t<0*. Substituting (3) in eqs. (1) and (2), we obtain

$$u_r = -\frac{1}{r^2}\int_r^\infty s\varphi(t-\frac{s-r_0}{c})ds \qquad (4)$$

$$\sigma_r = (\lambda+2\mu) - \frac{\varphi(t-\frac{r-r_0}{c})}{r} + \frac{4\mu}{r^3}\int_r^\infty s\varphi\left(t-\frac{s-r_0}{c}\right)ds \qquad (5)$$

Introducing the auxiliary function

$$\varphi(t) = \int_{-\infty}^{t} dt_2 \int_{-\infty}^{t_1} \varphi(t_1)dt_1 \qquad (6)$$

And integrating by part, the expressions (4) and (5) convert into the more suitable form

$$u_r = -\frac{c}{r}\varphi'\left(t-\frac{r-r_0}{c}\right) - \frac{c^2}{r^2}\varphi(t-\frac{r-r_0}{c}) \qquad (7)$$

$$\sigma_r = \frac{1}{r}\{(\lambda+2\mu)\varphi''\left(t-\frac{r-r_0}{c}\right) + \frac{4\mu c}{r}\varphi'\left(t-\frac{r-r_0}{c}\right) + \frac{4\mu c^2}{r^2}\varphi\left(t-\frac{r-r_0}{c}\right)\} \qquad (8)$$

For $r=r_0$the last equation yields

$$-P(t) = \sigma_{r\,(r=r_0)} = \frac{1}{r_0}\{(\lambda+2\mu)\varphi''(t) + \frac{4\mu c}{r_0}\varphi'(t) + \frac{4mc^2}{r_0^2}\varphi(t),$$

This together with the initial conditions deduced from (6)

$$\varphi(0) = \varphi'(0) = 0,$$

Determines *φ(t)*.

For the tangential stress σ_T perpendicular to the radius we find

$$\sigma_T = \lambda\theta + 2\mu\frac{u_r}{r} = \frac{1}{r}\{\lambda\varphi''\left(t-\frac{r-r_0}{c}\right) - \frac{2\mu c}{r}\varphi'\left(t-\frac{r-r_0}{c}\right) - \frac{2\mu c^2}{r^2}\varphi\left(t-\frac{r-r_0}{c}\right)\}$$

And consequently

$$\sigma_r + 2\sigma_T = \frac{1}{r}(3\lambda+2\mu)\varphi''(t-\frac{r-r_0}{c})$$

The quantity $r(\sigma_r+2\sigma_T)$ therefore moves unchanged with the velocity c.

If $P(t)=0$ for $t>t_0$, then

$$(\lambda+2\mu)\varphi''(t) + \frac{4\mu c}{r_0}\varphi'(t) + \frac{4\mu c^2}{r_0^2}\varphi(t) = 0 \quad (t>t_0)\,.$$

The solution is the damped vibration

$$e^{-\alpha t}\{A\sin\beta t + B\cos\beta t\}$$

$$\alpha = \frac{2\mu c}{r_0(\lambda+2\mu)}, \qquad \beta = \frac{2c\sqrt{\mu(\lambda+\mu)}}{r_0(\lambda+2\mu)}$$

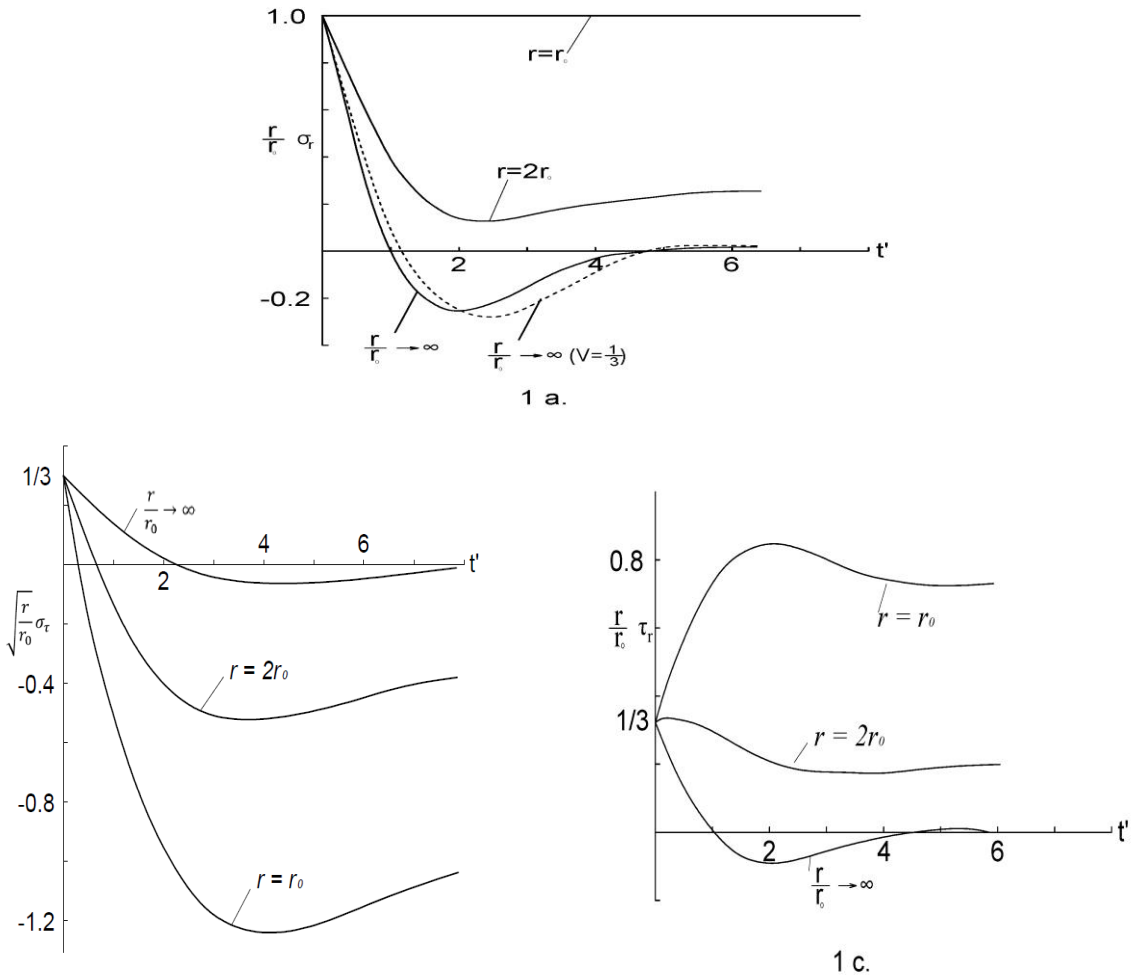

Figure 1: Spherical cavity. P (t)=-1. a. Radial stress. b. Tangential stress. c. Maximum shear stress

From eq.(8) is appears that a discontinuous jump of $\sigma_r$under propagation will decrease in proportion to $\frac{1}{r}$ with increasing distance r from the centre of the cavity, while in static equilibrium $\sigma_r$decreases in proportion to $\frac{1}{r^3}$. This applies even to the tangential stress.

Figures 1a, 1b and 1c show the redial stress σ_r, the tangential steressσ_T and the maximum shear stress τ multiplied by $\frac{r}{r_0}$ for different distances $r$at constant pressure $P(t)=-1$ at the boundary surface $r=r_0$ for $t>0$. The time parameter is

$$t' = \frac{ct}{r_0} - \frac{r - r_0}{r_0}$$

The calculations have been carried out for λ=μ corresponding to ν=$\frac{1}{4}$ (for granite ν=0.21-0.27[2].

1a. Radial stress (the dashed curve represents the radial stress at a great distance $\frac{r}{r_0} \to \infty$ for $\lambda=2\mu$, $\nu=\frac{1}{3}$

1b. Tangential stress.

1c. Maximum shear stress.

Transient Compression Wave from a Cylindrical Cavity

We now proceed to the case of a cylindrical cavity, the solid being defined by

$$r>r_0,\ r=\sqrt{x^2+y^2},\quad -\infty<z<\infty$$

At the time t=0 the solid is supposed to be in the unstressed state and at rest. After this time a uniformly distributed pressure $P(t)$ is supposed to be acting on the bounding surface $r=r_0$.

The displacement $u_r$takes place in the direction of the radius vector (x, y, 0) and putting

$$\Theta = \frac{1}{r}\frac{\partial (r u_r)}{\partial r} \qquad (9)$$

We find the radial stress $\sigma_r$equal to

$$\sigma_r = (\lambda + 2\mu)\Theta - 2\mu\frac{u_r}{r} \qquad (10)$$

Now

$$\nabla^2\Theta = \frac{\partial^2\Theta}{\partial r^2} + \frac{1}{r}\frac{\partial\Theta}{\partial r} = \frac{1}{c^2}\frac{\partial^2\Theta}{\partial t^2}$$

The Laplacian transform

$$\Theta^*(r,\xi) = \int_0^\infty \theta e^{-\xi t}\,dt$$

Accordingly satisfied the differential equation

$$\frac{\partial^2\theta^*}{\partial r^2} + \frac{1}{r}\frac{\partial\theta^*}{\partial r} = \frac{\xi^2}{c^2}\theta^*$$

$$\theta^* = \gamma(\xi)K_0\left(\frac{\xi\, r}{c}\right) \qquad (11)$$

$K_n(\xi)$ means the so-called second solution of the differential equation[3]

$$\xi^2 K'' + \xi K' - (\xi^2 + n^2)K = 0$$

Vanishing for $\xi\to\infty$ and related to the Hankel function $H_n^{(1)}(\xi)$ by the equation

$$K_n(\xi) = \frac{\pi i}{2}e^{\frac{1}{2}n\pi i}H_n^{(1)}(i\,\xi).$$

Introducing the Laplacian transform

$$\sigma^*(r,\xi) = \int_0^\infty \sigma e^{-\xi t}\,dt,$$

We obtain from (9) and (10)

$$\sigma^* = (\lambda + 2\mu)\theta^* + \frac{2\mu}{r}\int_r^\infty \theta^*\, r dr = \gamma(\xi)\{(\lambda + 2\mu)K_0\left(\frac{\xi\, r}{c}\right) + \frac{2\mu c}{r}K_1\left(\frac{\xi\, r}{c}\right)\}$$

Putting r=r_0, we find

$$\gamma(\xi) = \frac{\sigma^*(r_0,\xi)}{(\lambda+2\mu)K_0\left(\frac{\xi r_0}{c}\right)+\frac{2\mu c}{\xi r_0}K_1\left(\frac{\xi r_0}{c}\right)} \qquad (12)$$

And finally by inversion

$$\sigma_r = \frac{1}{2\pi i}\int_{u-i\infty}^{u+i\infty}\frac{(\lambda+2\mu)K_0\left(\frac{\xi\, r}{c}\right)+\frac{2\mu c}{\xi r}K_1\left(\frac{\xi r}{c}\right)}{(\lambda+2\mu)K_0\left(\frac{\xi r_0}{c}\right)+\frac{2\mu c}{\xi r_0}K_1\left(\frac{\xi r_0}{c}\right)}\sigma^*(r_0,\xi)e^{\xi t}\,d\xi \quad (u>0) \qquad (13)$$

If σ_a denotes the axial stress (in the zdirection), σ_T the tangential stress (perpendicular to the *z* axis and the radius vector (x,y,0), then σ_r, σ_T, σ_a constitute the principal stresses. Obviously

$$\sigma_a = \lambda\Theta$$
$$\sigma_T = \lambda\Theta + 2\mu\frac{u_r}{r}; \qquad (14)$$

Hence according to (10)

$$\sigma_r + \sigma_T = \frac{2(\lambda+\mu)}{\lambda}\sigma_a \qquad (15)$$

For the axial stress σ_a we deduce from eqs.(11),(12) and (14)

$$\sigma_a = \frac{1}{2\pi i}\int_{u-i\infty}^{u+i\infty}\frac{\lambda K_0\left(\frac{\xi r}{c}\right)\sigma^*(r_0,\xi)e^{\xi t}}{(\lambda+2\mu)K_0\left(\frac{\xi r_0}{c}\right)+\frac{2\mu c}{\xi r_0}K_1\left(\frac{\xi r_0}{c}\right)}d\xi \quad (u>0) \qquad (16)$$

In order to make expressions (12) and (16) easier to survey and more fitted for numerical calculations they will be brought into another form.

For the sake of simplicity it will be assumed in the following that $\sigma_{r\,(r=r_0)} = -P(t) = 1$ (constant tension =1 at r=r_0 for t>0). Then

$$\sigma^*(r_0,\xi) = \frac{1}{\xi} \qquad (17)$$

Now it can be proved, that the equation

$$F(\xi) \equiv (\lambda + 2\mu)K_0(\xi) + \frac{2\mu}{\xi}K_1(\xi) = 0 \qquad (18)$$

Has exactly one root $\xi_0=\alpha+i\beta$ in the half plane $\beta\geqq 0$ and that

$$\alpha < 0, \beta > 0$$

Inserting (17), we deduce from (13) and (16) after deforming the path of integration

$$\sigma_r = \frac{1}{\pi}\Im\int_0^{-\infty} \frac{F(\frac{\xi r}{r_0})e^{\frac{ct\xi}{r_0}}}{\xi\, F(\xi)}d\xi + 2\Re\frac{F(\frac{r\xi_0}{r_0})e^{\frac{ct\xi_0}{r_0}}}{\xi_0 F'(\xi_0)} + (\frac{r_0}{r})^2 \qquad (19)$$

$$\sigma_a = \frac{\lambda}{\pi}\Im\int_0^{-\infty} \frac{K_0(\frac{\xi r}{r_0})e^{\frac{ct\xi}{r_0}}}{\xi\, F(\xi)}d\xi + 2\lambda\Re\frac{K_0(\frac{\xi_0 r}{r_0})e^{\frac{ct\xi_0}{r_0}}}{\xi_0 F'(\xi_0)}; \qquad (20)$$

Here $\Im$ and $\Re$ mean imaginary and real parts.

Introducing in these equations the asymptotic expression

$$K_n(\xi) = \sqrt{\frac{\pi}{2\xi}}e^{-\xi}(1 + 0\left(\frac{1}{\xi}\right)) \qquad (21)$$

valid for $-\frac{3\pi}{2} < arg\xi < \frac{3\pi}{2}$ and letting $r/r_0 \to \infty$, we obtain after some simple transformations

$$\sqrt{\frac{r}{r_0}}\sigma_r == \frac{\lambda+2\mu}{\sqrt{2\pi}}\Im\int_0^{-\infty} \frac{e^{\frac{c\xi}{r_0}(t-\frac{r}{c})}}{\xi^{\frac{3}{2}}F(\xi)}d\xi + (\lambda+2\mu)\sqrt{2\pi}\Re\frac{e^{\frac{c\xi_0}{r_0}(t-\frac{r}{c})}}{\xi_0^{\frac{3}{2}}F'(\xi_0)} \quad (\frac{r}{r_0}\to\infty) \ (22)$$

$$\sqrt{\frac{r}{r_0}}\sigma_a = \frac{\lambda}{\lambda+2\mu}\sqrt{\frac{r}{r_0}}\sigma_r \qquad (\frac{r}{r_0}\to\infty) \qquad (23)$$

Hence

$$\sqrt{\frac{r}{r_0}}\sigma_T = \sqrt{\frac{r}{r_0}}\sigma_a \qquad (\frac{r}{r_0}\to\infty) \qquad (24)$$

We consider again eqs.(13) and (16).Inserting (17) corresponding to constant tension =1 at $r=r_0$ and letting $u\to\infty$, we obtain by means of (21) for $t = \frac{r-r_0}{c}+\varepsilon$ ($\varepsilon>0$)

$$\lim_{\varepsilon\to 0}\sigma_r = \lim_{\varepsilon\to\infty}\frac{1}{2\pi i}\int_{u-i\infty}^{u+i\infty}\sqrt{\frac{r_0}{r}}\frac{e^{\varepsilon\xi}}{\xi}d\xi = \lim_{\varepsilon\to\infty}\frac{\lambda+2\mu}{\lambda}\sigma_a$$

Thus, in the wave front

$$\sigma_r = \sqrt{\frac{r_0}{r}}$$

$$\sigma_a = \sigma_T = \frac{\lambda}{\lambda+2\mu}\sqrt{\frac{r_0}{r}} \qquad (25)$$

Letting $t\to\infty$, we receive from (19), (20) and (15)

$$\lim_{t\to\infty}\sigma_r = -\lim_{t\to\infty}\sigma_T = \left(\frac{r_0}{r}\right)^2$$

$$\lim_{t\to\infty}\sigma_a = 0$$

Hence, in static equilibrium the stresses decrease in proportion to r^{-2} with increasing radius r, while the stresses in the wave front decrease in proportion to r^{-t}, as can be seen from (25).

The numerical calculations, based upon the formulae of No.3 have been carried out under the supposition $\lambda = \mu$ ($\nu = \frac{1}{4}$). The root ξ_0 was calculated by successive approximation to

$$\xi_{0=}\text{-}0.442057+i0.447357$$

With a probable error $<10^{-4}$.

The figures show principal stresses, all multiplied by $\sqrt{r}/r_0$, for different distances *r* from the central axis. Unity of time *t* is chosen equal to the time which sound (velocity $c = \sqrt{\frac{\lambda+2\mu}{\varrho}}$) needs to travel the distance r_0 . The time parameter t' is

$$t' = t - \frac{r-r_0}{r_0}$$

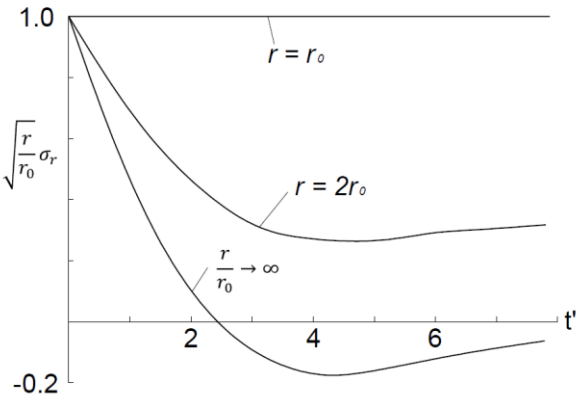

2 a.

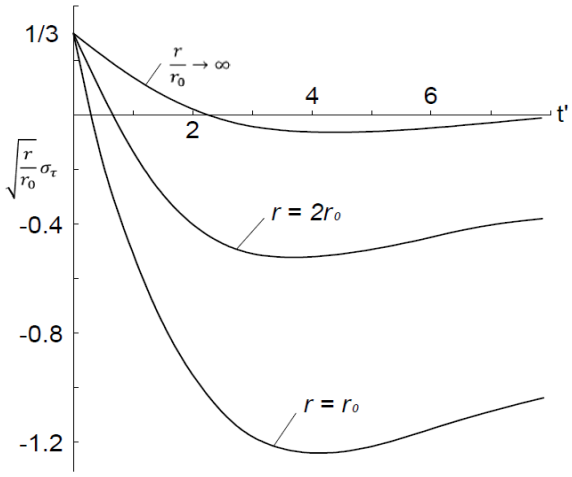

2 b.

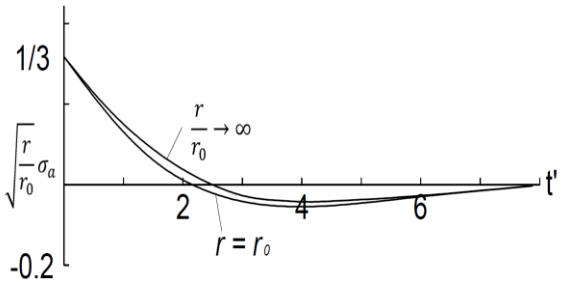

2 c.

Figures 2. Constant pressure P(t)=-1 at the boundary surface $r=r_0$ for t>0.

2 a. Radial stress.

2 b. Tangential stress.

2 c. Axial stress.

Conclusions

Under the influence of flat blast compression wave upon the solid inclusion with curved surfaces (borehole), whose dimensions are significantly smaller than the wavelength, and the wave propagation velocity in an inclusion`s material significantly higher, than in surrounding rocks, inclusion is slowly drown into a motion, at the same time the pressure on its rear side is equal to the pressure on the front side, and the coefficient of reflection of the wave from the front surface is approximately equal to 2.

Then, based on the Newton's second law, we can determine velocity of the inclusion U (t), as a rigid body. If the load on the inclusion is known, the strength calculation is carried out by known methods of structural mechanics. The above considerations allow us to show the physical nature of the impact of seismic waves on the frozen mud and freezing pipe.